

Seismic Response of Two 20-Story Reinforced Concrete Special Moment Frames Designed with Current Code Provisions



T. Visnjic, M. Panagiotou & J. P. Moehle

University of California – Berkeley, USA

SUMMARY:

This paper investigates numerically the two-dimensional (2D) seismic response of 20-story tall reinforced concrete (RC) special moment resisting frame (SMRF) buildings designed with current ASCE 7 and ACI 318 code provisions. Two SMRFs are considered. In the first, the column size and amount of reinforcement reduces with height, while the second frame has uniform column size and amount of column longitudinal reinforcement. The buildings are subjected to two sets of ground motions – one with pulse-type near-fault ground motions and another with far field non-pulse-type motions. Each of the sets is scaled so that its mean response spectrum matches the design basis as well as the maximum considered earthquake level spectra for a site located in Los Angeles, California. The study indicates that frames develop plasticity in the higher stories, and that design forces are greatly underestimated, especially in the exterior columns.

Keywords: Tall Buildings, Seismic Demand, Moment Frames, Reinforced Concrete Structures

1. INTRODUCTION

Construction of buildings exceeding 50m in height, referred herein as "tall" is increasing in earthquake-prone regions of the United States (U.S.) and worldwide (Emporis, 2012). Common structural systems used in the design of these buildings to resist strong earthquake excitations are reinforced concrete (RC) special moment resisting frames (SMRFs). Current design codes (ICC, 2009) have been calibrated primarily for low- to moderate-rise buildings and recent studies indicated that code-conforming prescriptive design of tall buildings may not produce a building that meets performance expectations during a design-basis earthquake (DBE) event (Krishnan, 2007, Haselton et al., 2011). In an effort to address deficiencies in design codes pertaining to response of tall buildings, several groups have developed procedures on establishing minimum performance expectations, design, and analysis requirements (LATBSDC 2005, SEAONC 2007, Moehle et al., 2008, Willford et al., 2008, TBI 2010, Moehle et. al., 2011). This study focuses on buildings where SMRFs are the only seismic lateral-load-resisting structural system.

In the case of RC SMRFs, the design forces are typically calculated using the modal response spectrum analysis (MRSA) method (ASCE, 2010) utilizing response modification factor $R = 8$ as code specified. The RC SMRF itself is subsequently detailed per the ACI 318 document. Numerical studies investigating the response of steel moment frames around 20 stories tall (Hall et al., 1995, Hall, 1998, Alavi and Krawinkler, 2004, and Krishnan, 2007) have indicated that strong pulse-type near fault excitations result in significant inelastic deformation demands which may be excessive and unattainable. The number of similar numerical studies of RC SMRFs is limited.

A numerical study on RC SMRFs by Haselton et al. (2011) included 12 to 20 story SMRFs and calculated an average probability of collapse of 11% for maximum considered earthquake (MCE) level earthquake excitation. This study indicated that satisfying current strong column – weak beam design requirements of ACI 318, does not always prevent the development of plasticity in the columns

above the base story. Barbosa (2011) showed that system shear demands in SMRFs exceed those predicted by current codes for DBE and MCE levels.

This paper investigates the seismic response of two 20-story tall RC SMRFs designed according to ASCE 7 and ACI 318 code provisions and subjected to strong earthquake excitation. Analytical models of the buildings are developed for nonlinear dynamic analysis under different sets of ground motions scaled to different hazard levels. Each set of ground motions has 14 records. The first set contains pulse-type near-fault ground motions and the second includes predominantly far-fault type records. Each set of ground motions considered in this paper is scaled to both the DBE as well as the MCE hazard levels. The results of analyses are quantified in terms of global response (story drifts, story shears, etc.) and local response (column shears, axial loads, and steel reinforcement strains).

2. BUILDING DESCRIPTION

The two buildings studied have the same elevation and plan view, shown in Figure 1. They utilize two reinforced concrete special moment resisting frames (SMRF) as a lateral-force-resisting system in each of the two principal directions. Each SMRF is placed at the perimeter and has four 6.4m long bays and 20 stories, each 3.66m tall. The total height, H , of both buildings is 73.2m. Column lines A and E (1 and 5) are designated “exterior columns,” column lines B and D (2 and 4) are designated “interior columns,” and column line C (3) is designated the “middle column” (refer to Figure 1).

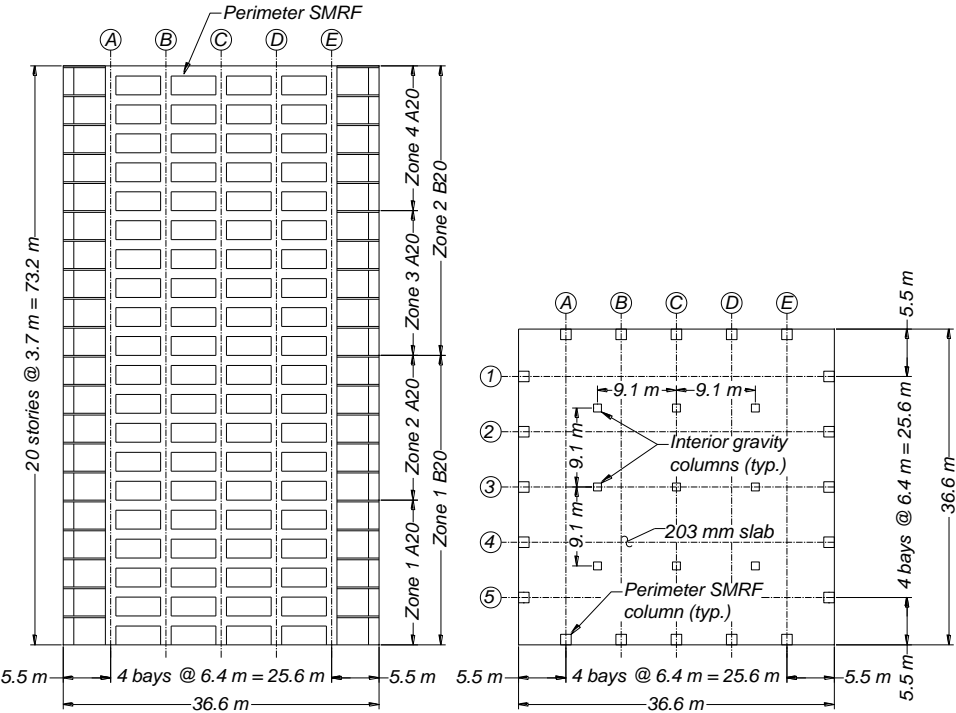


Figure 1. (Left) Elevation and (Right) floor plan of buildings considered

The first building, termed here A20-1, has a SMRF with columns and beams with varying size and longitudinal steel across the height. Levels 1-10 have uniform beam and column dimensions, 609mm x 1067mm and 1219mm x 1219mm, respectively. Levels 11-20 have smaller beams and columns, namely 609mm x 914mm and 1067mm x 1067mm, respectively. Column longitudinal steel reinforcement is curtailed at levels 6, 11 and 16. The second building, termed here B20-1, has uniform column size 1219mm x 1219mm and longitudinal reinforcement ratio equal to that used in the bottom stories of building A20-1 along its entire height. The beam size and reinforcement ratio distribution is identical to A20-1.

3. DESCRIPTION OF SEISMIC HAZARD AND GROUND MOTION SELECTION

The buildings considered in this study are located on a site in Los Angeles, CA with soil type D. Two sets of ground motions are selected and are each scaled to DBE as well as to MCE design spectra according to ASCE 7. The first set (Set 1) consists of 14 fault-normal components of near-fault pulse-type ground motions affected by directivity effects. The second set (Set 2) consists of 14 ground motions selected from a larger ground motion set (Baker et al., 2011) with source-to-site distance values ranging between 14 and 100 km and broad range of spectral amplitudes. The corresponding range of distance from the fault is 5 to 38 km. Figure 2(a) and (d) shows the mean acceleration spectra for the two sets of scaled ground motions together with the DBE and MCE smooth design spectra. The rest of Figure 2 shows individual scaled spectra of two ground motion sets for the DBE and MCE levels. These plots also show the vibration periods of the first two modes of the buildings, T_1 and T_2 , computed using uncracked material properties with the numerical model described in Section 5. Excellent agreement between the design spectra and the mean response spectra is observed for the periods between 0.5 and 4.0 seconds for both ground motion sets, which enfolds the said periods of vibration of the model buildings. Conditional mean response spectra (Baker, 2011) were not pursued because response of these tall buildings is strongly affected by multiple modes, and practical techniques using conditional mean spectra are not available for such cases.

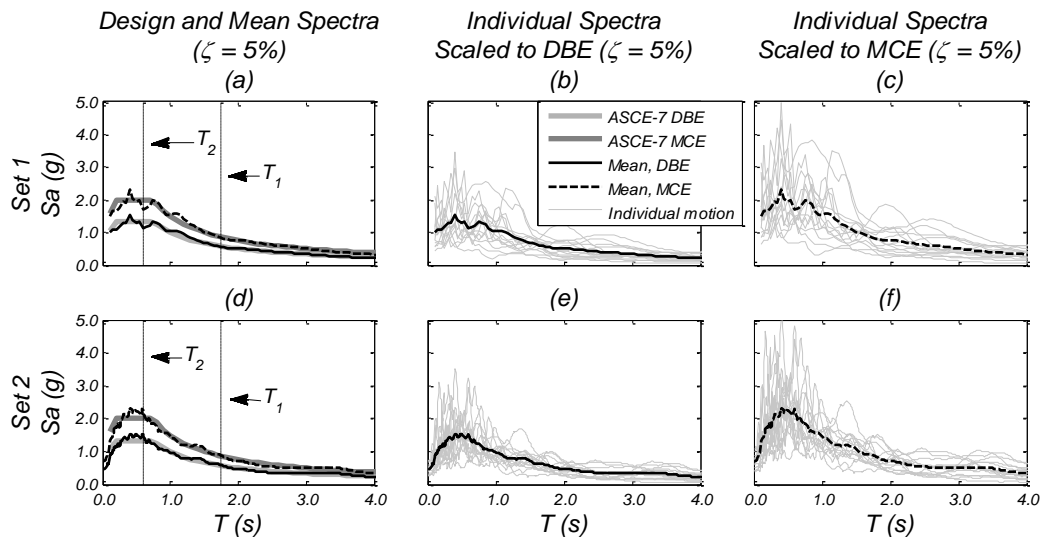


Figure 2. Design and linear pseudo-acceleration and displacement response spectra of ground motions scaled to DBE and MCE design seismic hazard levels (ζ = damping ratio)

4. DESIGN OF THE BUILDINGS

Buildings were designed based on ACI 318-11 and ASCE 7-10 provisions. Gravity loads were equal to 8.25 kN/m^2 and included the self-weight of structure and permanent non-structural components and contents. The design floor live load selected was 2.87 kN/m^2 . Total seismic weight of the two buildings, including 25% of the live load, was 233,000 kN and 238,000 kN for A20-1 and B20-1, respectively. The compressive strength of concrete, f'_c , was 52MPa, and steel tensile strength at yield, f_y , was 414MPa. Load combinations 1, 2, 5, and 7 as described in ASCE 7 were considered in the design. The buildings fall under occupancy category II, with importance factor $I = 1$ and seismic design category E. The design forces were determined using the code-prescribed modal response spectrum analysis (MRSa) with response modification factor $R = 8$. First five modes were included in the MRSa procedure, which included 90% of the modal mass. The design base shear force (V_b) for both buildings was controlled by minimum base shear force requirements of ASCE 7 resulting in a seismic response coefficient equal to $V_b / W = 5.36\%$, where W is the total seismic weight of the building.

The amount of longitudinal reinforcing steel in columns was reduced in building A20-1 every five stories. In the upper stories, the design was controlled by the minimum allowed longitudinal steel ratio $\rho_l = 1\%$. In building B20-1 the longitudinal steel ratio was uniform along the height. In both buildings, exterior columns had different design for interior and middle columns. Joint shear strength and strong column-weak beam requirements of ACI 318 were satisfied in both buildings. Transverse reinforcement in beams and columns of both buildings was designed to satisfy shear strength and confinement requirements of ACI 318.

5. NUMERICAL MODEL

The numerical analysis was performed on the Open System for Earthquake Engineering Simulation (OpenSees) platform (McKenna et al. 2007). The computer model consisted of a single SMRF with lumped mass and vertical load applied at the joints. Force-based Euler-Bernoulli nonlinear fiber-section frame elements with P- Δ geometric transformation were used to model all frame elements. The model accounted for the strain penetration of longitudinal reinforcement of beams in joints as well of the columns in the foundation. Foundation flexibility was not considered and columns were assumed fixed at the base. Initial stiffness Rayleigh damping with 2% damping ratio was applied in modes 1 and 3. The gravity framing is assumed to provide sufficient strength and stiffness to resist softening P- Δ effects under its gravity load on account of rigorous detailing requirements in new buildings. Moreover, Haselton et al. (2008) showed that the typical assumption of gravity system providing no lateral strength or stiffness was conservative. Therefore the P- Δ effects due to gravity framing were excluded from the numerical model.

6. RESULTS OF ANALYSIS

The buildings have similar modal characteristics with a first modal period $T_1 = 1.75$ s (1.76 s) and a ratio of first to second mode period $T_1 / T_2 = 2.87$; for both A20-1 and B20-1, the effective modal mass in the first, and second modes is over 73%, and 14%, respectively, of the total seismic mass, M , while the effective height of these modes is $0.7H$ for the first mode and $0.04H$ and $0.02H$ for the second mode of A20-1 and B20-1, respectively.

Figure 3 shows results of monotonic nonlinear static analysis, using the first-mode lateral force distribution up to 4% roof drift ratio. The buildings display almost identical force-displacement relationship, with an approximate system base shear of $0.08W$ at 0.5% roof drift ratio, and $0.10W$ at 4% roof drift ratio. At 2% roof drift, the base shear is $0.09W$ which is 67% higher than the design base shear of $0.054W$ due to design and section overstrength. Figure 3 also shows instances when the tensile strain in steel of base exterior column on the uplift side reaches strain levels of 1, 2, and 4%.

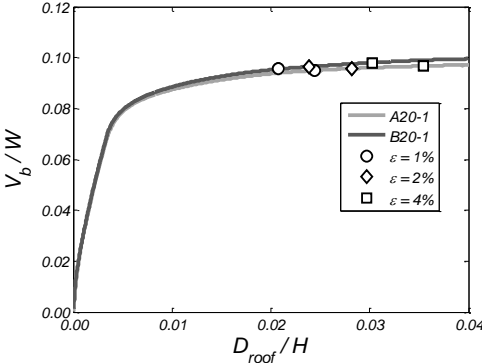


Figure 3. Force-displacement curves from first-mode force distribution pushover analysis

6.1. Nonlinear Response History Analysis of A20-1 for Ground Motion Set 1

The results of the NRHA are first discussed for ground motion Set 1 consisting of near-fault, pulse-type ground motions. Representative response quantities are plotted in terms of the computed mean response to the 14 ground motions. Figure 4 plots: (a) mean envelopes of relative displacements, D , normalized with H , (b) floor accelerations normalized with ground motion peak ground acceleration, PGA , (c) inter-story drifts, θ , (d) story moments normalized with WH , and (e) and (f) story shear forces normalized with W for A20-1 and B20-1, respectively.

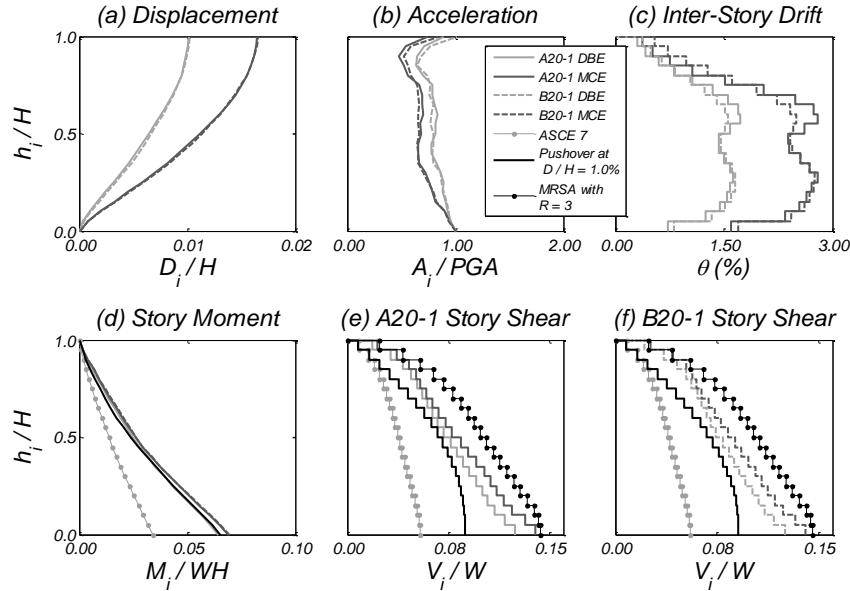


Figure 4. System mean response parameter envelopes for A20-1 and B20-1 buildings and near fault, pulse-type ground motion set scaled to DBE and MCE

The envelopes of all response quantities for DBE and MCE levels have similar shapes. The computed mean roof drift ratio for building A20-1 was 1.0 and 1.6% at DBE and MCE levels, respectively. As shown in Figure 4, the mean drift envelopes had a peak value at the roof of the building and increased by approximately 1.6 from DBE to MCE level. The average inter-story drift along the building height was 1.23% and 2.03% for the DBE and MCE level, respectively. The peak values of the mean inter-story drift envelopes for the DBE and MCE were 1.7% and 2.8% and occurred at about 60% of the building height. They were almost constant below this location. The increase in inter-story drifts between DBE and MCE levels was about 1.65 times.

The mean base shear force at the DBE was $0.12W$ and increased to $0.14W$ at MCE hazard level. As shown in Figure 4, the mean base shear force at DBE is 33% higher than the base shear force computed from a monotonic nonlinear static analysis using the first model lateral force profile at 1.0% roof drift ratio which is equal to the mean roof drift ratio for the DBE level. This difference is due to contributions from higher modes, and especially of the second mode, which is evident from the story shear distribution from first-mode pushover analysis plot at a mean roof drift ratio, plotted in Figure 4(e). Modified MRSA analysis using a trial-and-error obtained value of $R = 3$ provides a better estimate of the system shear, as can be observed in Figure 4(e). An almost negligible difference exists in the mean computed story moments between the two hazard levels; see Figure 4(d). This is because most of the story moment contribution comes from the moment couple of axial column forces, which did not show significant difference for the two hazard levels.

Significant inelastic strains developed in the frame members at both the DBE and the MCE shaking level. The average beam reinforcement tensile strain along the height of the buildings was 4.3%, and 5.6%, at the DBE and MCE level respectively. As Figure 5 shows, the mean reinforcement tensile

strain envelopes of the beams have a peak value of 6.8%, and 7.9% at the DBE and MCE level, respectively. The strain envelopes at both seismic hazard levels have similar shapes with nearly uniform strain levels in the bottom 70% of the height of the building.

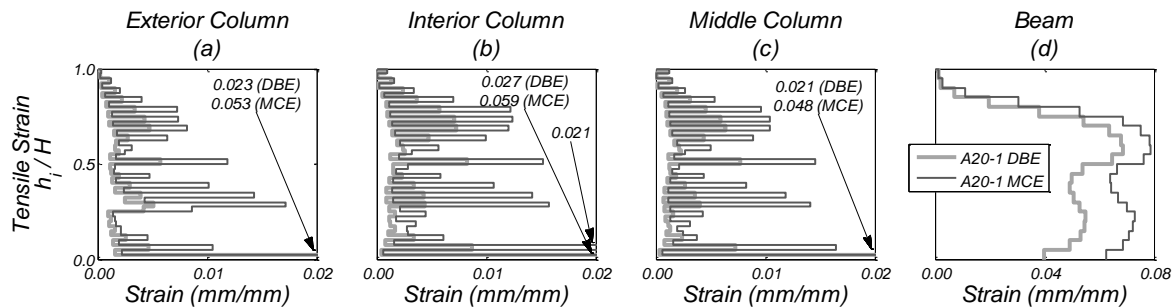


Figure 5. Mean reinforcement tensile steel strain envelopes in columns and beams of building A20-1 subjected to pulse-type ground motion set at two levels of shaking

As can be observed in Figure 5(a) – 5(c) for both DBE and MCE levels, significant inelastic deformations are developed in the columns with peak reinforcement tensile strains computed at the base of the bottom story. The mean reinforcement tensile strain at the base of exterior column for the DBE (MCE) level was 2.3% (5.3%). Inelastic deformations developed above the bottom story in all columns, which is especially evident at the MCE level response (Figure 5). The interior column developed roughly 30% larger reinforcement tensile strains than the exterior column, over the building height. At the DBE, the mean reinforcement tensile strains above the base in the exterior columns were less than 0.6%, while at the MCE level they reached up to 1.8%. At MCE level, mean tensile strains at the locations of interior column size and longitudinal reinforcement curtailment level, $0.25H$, $0.50H$ and $0.75H$, were 1.6, 1.5, and 1.2%, respectively (see Figure 5).

Figure 6(a) shows the axial force envelope of the exterior columns, P , normalized by $f'_c A_g$, (A_g = gross area of the member). The axial forces increase less than 5% from DBE to the MCE level. NRHA results indicate that axial forces in exterior columns exceed the design forces calculated by code procedures. The primary source of this difference is that the latter do not account for the design overstrength due to the as-designed flexural strength of columns and beams. Section hardening of the beams along the height of the building with increase of lateral displacements is the second reason resulting in an increase of the axial forces. Based on the pushover analysis at 0.5% roof drift ratio, the tension and compression force at the base of the exterior columns were 1.64, and 1.23 times larger than that obtained from MRSA. The mean tensile force computed at the base of the exterior columns in NRHA was higher than MRSA-calculated values 1.83 times for the DBE level and 2.06 for the MCE level of shaking. The corresponding values for the mean compressive force in the exterior columns at the base are 1.28 and 1.35 times the forces calculated by MRSA for the DBE and MCE, respectively.

Lastly, individual column shear envelopes normalized by $A_g \sqrt{f'_c}$ (f'_c in MPa) are plotted in Figure 6(b) through (d), along with the design forces calculated by five different methods for the exterior, interior, and middle column, respectively. The shear forces computed using NRHA exceeded those computed using MRSA more than 2 times on average along the height. The first-story exterior column developed 1.41 and 1.59 times higher peak shears than the first-story interior and middle columns, respectively (Figure 6). Inelastic flexural deformations of the beam result in beam elongation that forces the exterior columns outward (Qi and Pantazopoulou, 1991, Fenwick and Megget, 1993, Kim et al., 2004). This results in an increase of the shear force as well as rotation the exterior column that exhibits increased compression during lateral deformation of the building. Note that while the shear force at the base of the third story of the interior column is 58% larger than the corresponding shear of the exterior column, the latter experiences 40% larger shear at the base than the interior column, at DBE hazard level.

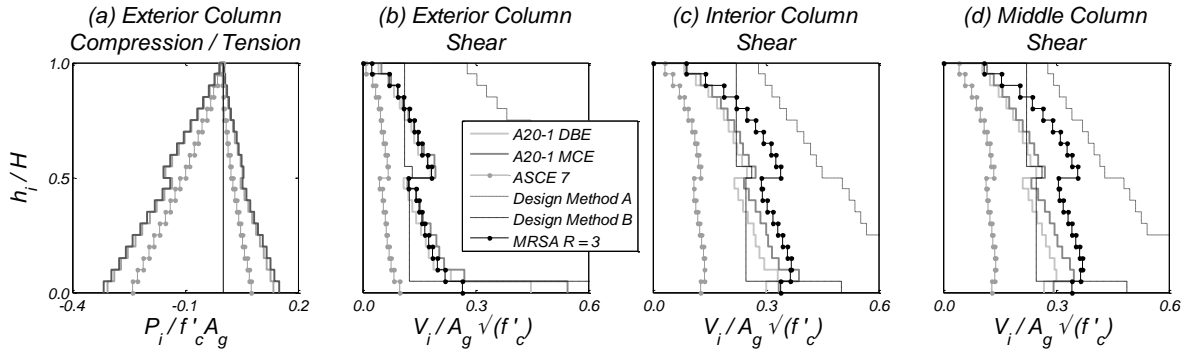


Figure 6. Mean response envelopes for exterior column axial loads and column shear in exterior, interior, and middle column for buildings A20-1 and the near-fault, pulse-type ground motions, at two levels of shaking.

Two methods specified in ACI 318-11 for calculating shear force demands are considered. Method A considers the shear V_i developed in the column at the time when both of its ends reach the maximum probable moment strength, $M_{pr,c}$, associated with the range of factored axial loads, P_u , calculated from the appropriate load combinations (ASCE 7). That is, $V_i = 2M_{pr,c,i} / l_{u,i}$ where l_u is the column clear height. Method B considers column shear at the instant when beams framing into the joint develop their respective probable moment strengths, $M_{pr,b}$, but the resisting moments in column above and below are indeterminate and it is up to a designer to decide the moment distribution pattern. It is not uncommon in practice to assume the resisting moment $\sum M_{pr,b}$ at a given joint to be divided evenly between the column above and below the joint. This gives a design shear at floor $i > 1$, $V_i = (\sum M_{pr,b,i} + \sum M_{pr,b,i-1}) / 2l_{u,i}$. In the first story, column design shear is obtained by replacing the $\sum M_{pr,b,i}$ values by the column $M_{pr,c}$ at level $i - 1$, that is, at the base of the building.

Method A significantly overestimated the shear force demands compared to those computed using NRHA for all columns along the height (Figure 6). Shear forces calculated by this method at the base of the columns were between 2.2-2.5 times the mean shear forces computed by the NRHA for the MCE hazard level. Method B underestimated the shear forces in all columns along most of the bottom two-thirds of the building height. The exception was at the bottom story where Method B resulted in shear forces 1.2, 1.5, and 1.6 times the mean shears computed by the NRHA for the MCE level in the exterior, interior, and middle columns, respectively.

Modified MRSA with $R = 3$ provides a better estimate for the shear forces in interior and middle column, except at the top story and the second story of interior column. Exterior column shear force demand at MCE seismic hazard exceeds the design forces calculated by this method across all of the building height. Exterior column shear force at the bottom two floors computed by NRHA at DBE exceeds that calculated by modified MRSA, due to beam growth not explicitly taken into account in design.

6.2. Nonlinear Response History Analysis of B20-1 for Ground Motion Set 1

The analyses of building B20-1 under ground motion Set 1 and Set 2 showed very similar results to those of A20-1 except the tensile strains of the columns above the sixth story which was the first level of column size and longitudinal steel curtailment in buildings A20-1. The mean and peak roof drift ratios, base shear forces, axial forces at the base of the exterior columns, and beam tensile strains were practically same to those of A20-1, see comparison of mean envelopes in Figure 4.

Contrary to column reinforcing steel strain levels in A20-1, the mean longitudinal steel strains in columns at levels 6, 11, 16 of B20-1 reached, but did not exceed yielding strains for the DBE motions. At the MCE levels, the mean strain in these levels reached 0.7, 0.2, and 0.4% for the interior, 0.6, 0.2, and 0.4% for the middle column, respectively. Tensile strains recorded in the exterior column were 0.2% at all three locations. Beam and column strains are plotted in Figure 7.

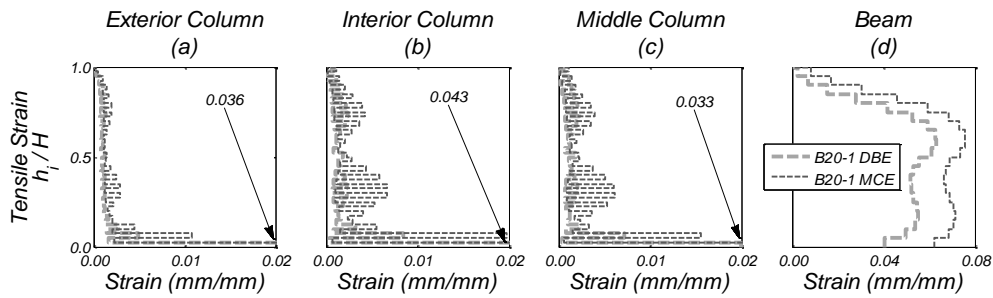


Figure 7. Mean tensile steel strain envelopes in columns and beams of building B20-1 subjected to pulse-type ground motion set at two levels of shaking

Shear forces in individual columns display the same trends as those in building A20-1, and are not plotted here. Column shear is underestimated by Method B. Modified MRSA with $R = 3$ provides a good estimate of mean shear forces in the interior and middle columns across most of the building height, but underestimates the forces in the exterior columns everywhere.

6.3. Nonlinear Response History Analysis of Frames for Ground Motion Set 2

Both buildings display little difference in mean response envelopes between the near-field pulse-type and far-field type motions. Selected response quantities are plotted in Figure 8 for A20-1 building only. This figure also shows the mean response envelopes for Set 1. Slightly increased floor accelerations are noted at both hazard levels for ground motion Set 2. Larger inter-story drifts are shifted to the upper half of the building, while they are decreased in the lower half for both DBE and MCE shaking intensities. Tensile strains (not shown here) in columns of A20-1 building follow similar distributions for both ground motion sets, with spreading of plasticity in columns across the building height, while for B20-1 column plasticity is contained only at the bottom of the building at DBE.

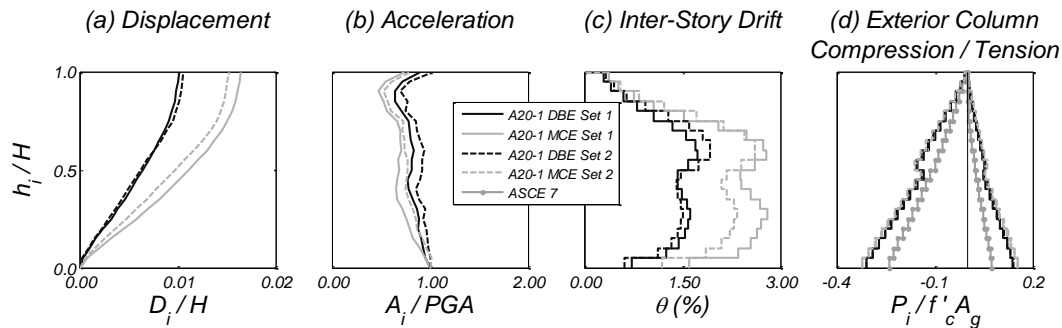


Figure 8. Comparison of mean response envelopes of A20-1 for ground motion Set 1 and Set 2

7. CONCLUSIONS

The study investigated the seismic response of two 20-story reinforced concrete special moment resisting frames, described in Sections 3 and 4. The buildings were subjected to two sets of ground motions, each scaled to DBE and MCE design spectra, for a site located in Los Angeles, CA. Based on the results previously presented the following conclusions are drawn:

- 1) For both DBE and MCE hazard levels, both buildings developed significant inelastic deformations in the columns at the base of the building and in the beams along the bottom 60% of the building height. The mean strain levels at the base of the column were the largest in the interior columns in both buildings. While the strain values at the column base have similar values in the two buildings, notable difference is observed in the strain distribution pattern along the building height.

2) The A20-1 building developed inelastic deformations in the columns above the base of the building in the levels where the flexural strength of the columns reduced significantly. The mean tensile strains in interior columns at stories 6, 11, and 16 and at DBE shaking intensity were 0.4, 0.8, and 0.6% respectively. At the MCE shaking level they were 1.6, 1.5, and 1.2% at the three locations, respectively. In building with uniform column section the strain levels at the corresponding locations were under yielding value for the DBE and slightly higher than yielding at MCE.

3) Equivalent elastic analysis significantly underestimates axial forces in the columns. The mean axial tensile force in exterior columns of A20-1 was 1.83 and 2.06 times the value computed by the code prescribed procedure for the DBE and MCE hazard levels, correspondingly. In the case of compressive force, the exterior column recorded 1.28 and 1.35 times the axial compression estimated by the code. In building B20-1, these values were 1.87 and 2.09 for tension at DBE and MCE, respectively. For compression, the mean axial force computed was 1.27 and 1.33 times the code-estimated value at the two levels of intensity, respectively.

4) As a result of higher mode effect contribution to the system shear, the equivalent elastic analysis provides non-conservative estimation of column shear forces. The mean shear force developed in the exterior columns of A20-1 was 4.13 times the shear calculated by the elastic analysis in the case of the DBE hazard level and 5.07 times the same value for the MCE level. For B20-1, the mean shear computed in exterior columns was 4.06 times the value estimated by the elastic analysis at DBE, and 5.03 for the MCE. Use of modified response modification factor R may provide a closer estimate of shear forces in columns, with the exception of the region at the base of exterior columns.

5) Current state-of-practice method used for shear design of columns underestimates the shear forces. Common interpretation of Method B described in Section 6.1 and defined in ACI-318 resulted in exterior column shear force at the base of the building 0.3 and 0.24 times the mean recorded shear at DBE and MCE levels, correspondingly. In the interior column at the base the design shear calculated by this method was 0.84 and 0.74 times the mean recorded for the DBE and MCE, respectively.

6) Kinematic interaction between beams and columns at the base significantly affects the shear force distribution among the base columns. The mean shear force in the exterior columns at the base of the buildings was between 1.42 and 1.58 times larger than the mean shear force in the interior columns. The equivalent elastic analysis (MRSA) does not account for this effect and will always result in the underestimation of the shear demand in exterior columns at the base.

7) Little difference is noted in mean system responses between the two ground motion sets. Both near-field pulse-type motions and combined set ground motions cause concentration of plasticity in the upper stories in the building A20-1.

ACKNOWLEDGEMENT

The study presented was conducted as part of the Tall Buildings Initiative of the Pacific Earthquake Engineering Research Center, University of California, Berkeley.

REFERENCES

- Alavi, B. and Krawinkler, H., 2004. Behavior of Moment-Resisting Frame Structures Subjected to Near-Fault Ground Motions, *Earthquake Engineering and Structural Dynamics*, **33**.687–706.
- American Concrete Institute (ACI), 2011. *BuildingCode Requirements for Structural Concrete, Tech. Rep. ACI-318*, Farmington Hills, MI.
- American Society of Civil Engineers (ASCE), 2010. *Minimum design loads for buildings and other structures, Tech. Rep. ASCE 7-10*, Reston, VA.
- Baker, Jack W., 2011. Conditional Mean Spectrum: Tool for Ground-Motion Selection, *ASCE Journal of Structural Engineering*, **137**.322-331.

- Baker, Jack W., Lin, Ting, Shahi, Shrey K., 2011. New Ground Motion Selection Procedures and Selected Motions for the PEER Transportation Research Program, Tech. Rep. PEER 2011/03 Pacific Earthquake Engineering Research Center, Berkeley, CA.
- Emporis, 2012. Building database. <http://www.emporis.com/statistics/>.
- Fenwick, R.C., Megget, L. M., 1993. Elongation and Load Deflection Characteristics of Reinforced Concrete Members Containing Plastic Hinges. *New Zealand National Society for Earthquake Engineering*, **26**.28-41.
- Hall J.F., Heaton, T.H., Halling, M.W., and Wald, D.J., 1995. Near-Source Ground Motion and its Effects on Flexible Buildings, *Earthquake Spectra*, **11**.569-605.
- Hall, J.F., 1998. Seismic Response of Steel Frame Buildings to Near-Source Ground Motions, *Earthquake Engineering and Structural Dynamics*, **27**.1445-1464.
- Haselton, C.B., Goulet, C.A., Mitrani-Reiser, J., Beck, J.L., Deierlein, G.G., Porter, K.A., Stewart, J.P., and Taciroglu, E., 2008. An Assessment to Benchmark the Seismic Performance of a Code-Conforming Reinforced Concrete Moment-Frame Building, Tech. Rep. PEER 2007/12 Pacific Earthquake Engineering Research Center, Berkeley, CA.
- Haselton, C.B., Liel A.B., Deierlein, G.G., Dean, B.S., Chou, J.H., 2011. Seismic Collapse Safety of Reinforced Concrete Buildings: I. Assessment of Ductile Moment Frames, *ASCE Journal of Structural Engineering*, **137**.481-491.
- International Code Council (ICC), 2009. *International Building Code*, International Code Council, Falls Church, VA.
- Kim, J., Stanton, J., and MacRae, G., 2004. Effect of Beam Growth on Reinforced Concrete Frames, *ASCE Journal of Structural Engineering*, **130**.1333-1342.
- Krishnan, S., 2007. Case Studies of Damage to 19-storey Irregular Steel Moment-Frame Buildings under Near-Source Ground Motion, *Earthquake Engineering and Structural Dynamics*, **36**.861–885.
- Los Angeles Tall Buildings Structural Design Council (LATBSDC), 2005. *An Alternative Procedure for Seismic Analysis and Design of Tall Buildings Located in the Los Angeles Region*, Los Angeles Tall Buildings Council, Los Angeles, CA.
- McKenna, F., Fenves, G. L., and Scott, M. H., 2007. Open System for Earthquake Engineering Simulation (OpenSees). Pacific Earthquake Engineering Research Center, <http://opensees.berkeley.edu/>.
- Moehle, Jack P., Hooper, John D., and Lubke, Chris D., 2008. Seismic Design of Reinforced Concrete Special Moment Frames: A Guide for Practicing Engineers. *NEHRP Seismic Design Technical Brief No.1*, NIST GCR 8-917-1.
- Moehle J.P., Bozorgnia, Y., Jayaram, N., Jones, P., Rahnama, M., Shome, M., Tuna, Z., Wallace, J.A., Yang, T.Y., Zareian, F., 2011. Case Studies of the Seismic Performance of Tall Buildings Designed by Alternative Means. Task 12 Report for the Tall Buildings Initiative. Tech. Rep. PEER 2011/05 Pacific Earthquake Engineering Research Center, Berkeley, CA.
- Qi, X., Pantazopoulou, S. J., 1991. Response of RC Frame under Lateral, *ASCE Journal of Structural Engineering*, **117**.1167-1188.
- Structural Engineers Association of Northern California (SEAONC), 2007. *Seismic Design and Review of Tall Buildings Using Non-Prescriptive Procedures*, Recommended Administrative Bulletin, SEAONC, San Francisco, CA.
- TBI Guidelines Working Group, 2010. Guidelines for Performance-Based Seismic Design of Tall Buildings, Tech. Rep. 2010/05 Pacific Earthquake Engineering Research Center, Berkeley CA.
- Willford, M., Whittaker, A., Klemencic, R., 2008. *Recommendations for the Seismic Design of High-Rise Buildings*, Council on Tall Buildings and Urban Habitat (CTBUH), Chicago, IL.